THE JOURNAL OF PHYSICAL CHEMISTRY B

Article

2D ^{1}H/^{1}H RFDR and NOESY NMR Experiments on a Membrane-Bound Antimicrobial Peptide Under Magic Angle Spinning

Ayyalusamy Ramamoorthy* and Jiadi Xu

Biophysics and Department of Chemistry, The University of Michigan, Ann Arbor, Michigan 48109-1055, United States

ABSTRACT: There is significant interest in solving high-resolution dynamic structures of membrane-associated peptides using solid-state NMR spectroscopy. Previous solid-state NMR studies have provided valuable insights into the functional properties of an exciting class of biomacromolecules such as antimicrobial peptides and amyloid peptides. However, it has been a major challenge to apply solid-state NMR techniques to study peptides or proteins that are not labeled with specific isotopes such as ^{13}C, ^{15}N, and/or ^{2}H. This study utilizes 2D ^{1}H/^{1}H radio frequency-driven recoupling (RFDR) and nuclear Overhauser effect spectroscopy (NOESY) pulse sequences under magic angle spinning to study a membrane-bound antimicrobial peptide MSI-78 (or also known as pexiganan). We demonstrate that proton resonances can be assigned and structural constraints, NOE and ^{1}H−^{1}H dipolar couplings, can be measured without the need for any isotopic enrichment. The buildup curves, showing the dependence of the cross peak intensity against the mixing time, obtained from 2D ^{1}H/^{1}H NOESY and RFDR experiments are compared. Our results reveal that the RFDR-recovered ^{1}H−^{1}H dipolar couplings associated with alpha and side chain protons are larger than that with the amide-protons. This study provides a means to measure residual ^{1}H−^{1}H dipolar couplings for the investigation of structure, dynamics, and aggregation of peptides using a suitable model membrane like micelles or bicelles.

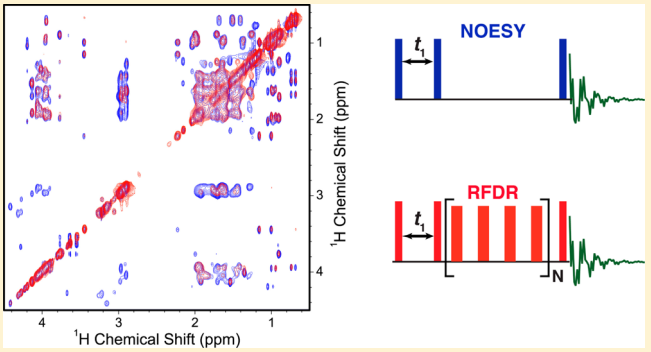

INTRODUCTION

Structure determination of peptides and proteins by NMR (nuclear magnetic resonance) spectroscopy frequently uses two types of parameters: nuclear Overhauser effect (NOE)[1−3] and dipolar coupling.[4−7] For the structural studies of membrane-associated peptides, nuclear Overhauser effect spectroscopy (NOESY) experiments[8] on micelles are used to measure NOEs whereas solid-state NMR experiments are utilized in the measurement of dipolar couplings.[7] Studies have shown that weakly aligned samples can be used to measure residual dipolar couplings (RDC).[4,6,9] Though these approaches have been successfully applied to solve high-resolution structures of membrane-associated proteins, there are challenges in the structure determination of membrane-bound peptides that cannot be expressed in bacteria. Site-specific labeling (example, ^{13}C, ^{2}H and/or ^{15}N isotopes) is essential for studies on such systems using solid-state NMR spectroscopy, although crystalline/homogeneous samples containing uniformly labeled peptides can be investigated using magic angle spinning (MAS) experiments.[10−15] On the other hand, aggregating peptides (like amyloid or antimicrobial peptides) may not be sufficiently small to be studied by solution NMR spectroscopy;[16,17] ^{1}H−^{1}H dipolar couplings incompletely averaged by the slow motion lowers the resolution of proton spectral lines and also interfere with the observed NOE effects; in this study, we refer to these unaveraged small dipolar couplings as "residual dipolar couplings"; it should not be confused with the RDCs used in the study of aligned samples as mentioned above.[4,6,9] Under such conditions, the traditional total correlation spectroscopy (TOCSY)[18] experiment also fails due to short spin−spin relaxation, T_2, of protons. On the other hand, the residual (or unaveraged) dipolar coupling itself contain important structural information and if measured they could be utilized in the structure and dynamics studies using NMR spectroscopy.

Here, we report a study that can be used to measure the residual ^{1}H−^{1}H dipolar couplings directly from a model membrane containing MSI-78 peptide without the need for aligning the sample. The commercial name of MSI-78 is pexiganan and the amino acid sequence GIGKFLKKAKKKFG-KAFVKILKK. It is an antimicrobial peptide developed to treat diabetic foot ulcer infections.[19] It has been demonstrated that MSI-78 exhibits a broad-spectrum of antimicrobial activities against both Gram-positive and Gram-negative bacteria.[20,21] In the NMR approach utilized in this study to investigate the membrane interaction of MSI-78, dipolar couplings are completely suppressed by applying MAS to obtain high-resolution ^{1}H spectra. Then, the ^{1}H−^{1}H dipolar couplings are reintroduced using the radio frequency-driven recoupling (RFDR) pulse sequence.[22] This pulse sequence was previously demonstrated on a DMPC (1,2-dimyristoyl-sn-glycero-3-phosphocholine) lipid bilayer sample.[23] The rate of relaxation

Received: April 6, 2013
Revised: May 14, 2013

   dx.doi.org/10.1021/jp4034003 | J. Phys. Chem. B XXXX, XXX, XXX−XXX

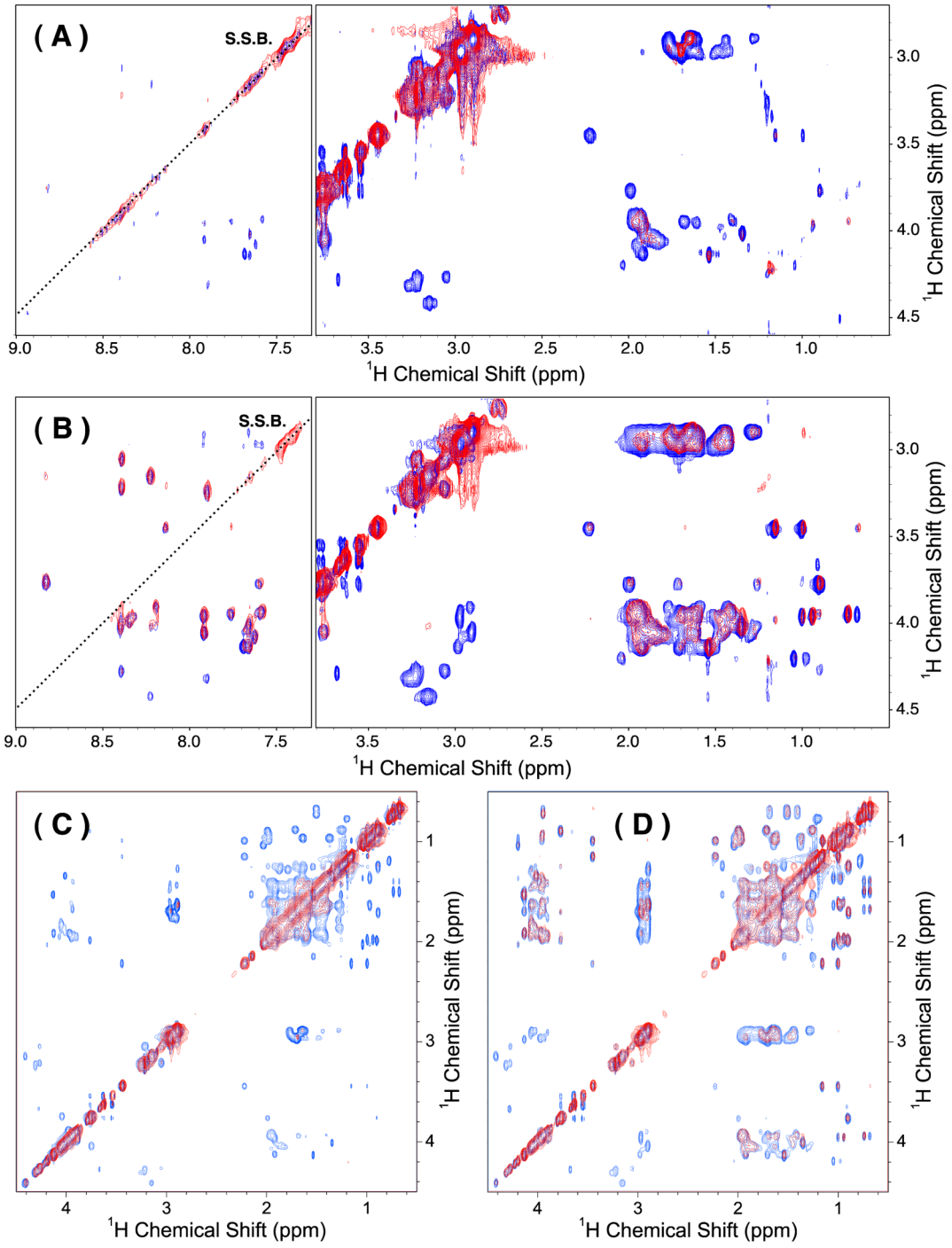

Figure 1. 2D ^{1}H/^{1}H NOESY (red) and RFDR (blue) spectra of MSI-78 embedded in DPC micelles obtained under MAS conditions recorded at two different mixing times: 50 ms (A and C) and 100 ms (B and D). The spinning side bands (ssb) are indicated using dotted lines.

times are reduced for protons and the spectral lines are narrowed due to the suppression of line broadening anisotropic interactions by MAS; the high-resolution spectra render the assignment of all ^{1}H peaks observed in 2D NOESY and RFDR spectra obtained under MAS. A detailed analysis of the NOEs and residual dipolar couplings measured under MAS condition is presented. We believe that this approach can be used to study the membrane-bound structures of polypeptides without the need for isotopic labeling.

MATERIALS AND METHODS

NMR Samples. A 22-residue antimicrobial peptide MSI-78 was used in this study. The NMR samples were prepared by dissolving the lyophilized peptide in an aqueous solution (10% D_2O and 90% H_2O) containing 150 mM perdeuterated DPC (purchased from Cambridge Isotope Laboratory) and 20 mM phosphate buffer at pH ~7 to make a final concentration of 2 mM. The total sample volume used in NMR measurements was 40 μL.

NMR Spectroscopy. All NMR measurements were performed at 35 °C on a Agilent/Varian VNMRS 600 MHz

dx.doi.org/10.1021/jp4034003 | J. Phys. Chem. B XXXX, XXX, XXX−XXX

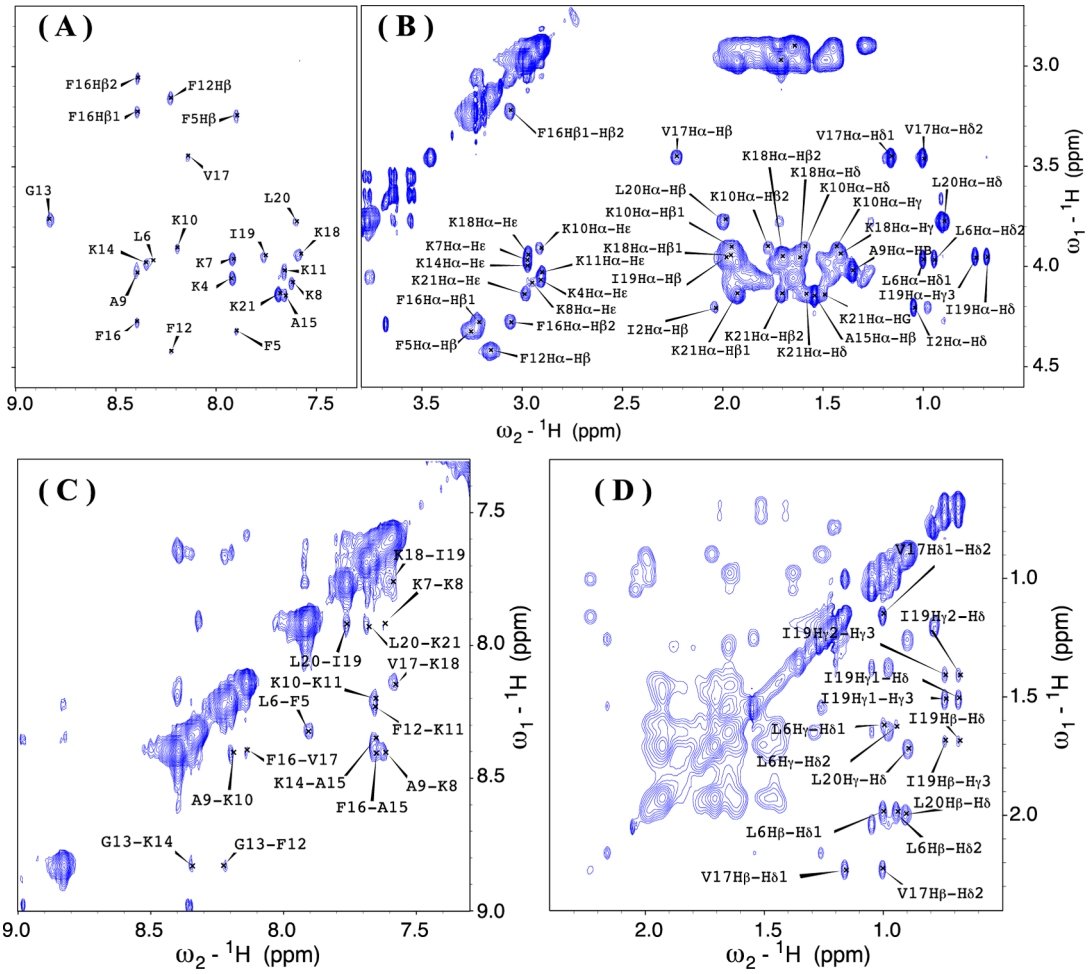

Figure 2. The peak assignments for the 2D $^1H/^1H$ RFDR spectrum of MSI-78 embedded in DPC micelles. The spectra were obtained under MAS conditions using a 100 ms mixing time. Panels A–D are the zoomed view of the 2D RFDR spectra for the clarity. The peak assignments were achieved using NOESY spectra obtained at different mixing times. NOESY spectra obtained using longer (100 ms) and shorter (50 ms) mixing times were used for inter-residue and intraresidue assignments, respectively.

solid-state NMR spectrometer using a 4 mm $^1H/X$ double-resonance nanoprobe. The spectrometer was operated with a deuterium field lock and samples were spun at 2.7 kHz. All samples were equilibrated at 35 °C for a period of ~30 min prior to NMR measurements. The proton carrier frequency was set at the water resonance for all experiments and ^1H_2O resonance was suppressed using a 50 Hz RF pulse for 1s at the beginning of the NOESY and RFDR pulse sequences. The radio frequency field strength used for the 90 and 180° pulses was 83 kHz. The 2D NOESY and RFDR spectra were recorded using 400 t1 increments and 512 t2 complex points. The experimental data sets were zero-filled in both the t1 and t2 dimensions to form a 1024 × 1024 data matrix. Phase-shifted sine bell multiplication was applied in both dimensions prior to Fourier transformation. The NMR data were processed using NMRPipe[24] and analyzed using Sparky.[25] Assignment of proton resonances was accomplished by using 2D $^1H/^1H$ NOESY spectra obtained at 50 and 100 ms mixing times.

RESULTS AND DISCUSSION

Assignment of Resonances in 2D RFDR and NOESY Spectra of MSI-78 Embedded in DPC Micelles. As mentioned in the previous section, 2D $^1H/^1H$ NOESY and RFDR experiments were performed on DPC micelles containing MSI-78 (Figure 1). As discussed below, few cross peaks were observed in the amide-NH region (Figure 1A,B). On the other hand, strong cross peaks can be seen for the aliphatic protons (Figure 1C,D). Resonances were assigned using 2D NOESY spectra obtained at two different mixing times (Figure 2). A NOESY spectrum obtained using a short mixing time (50 ms) was used, instead of a 2D TOCSY spectrum, to identify the amino acid types. On the other hand, a NOESY spectrum obtained using a long mixing time (100 ms) was used for the inter-residue sequential assignment. Combining these two 2D $^1H/^1H$ NOESY spectra, backbone, and side-chain proton resonances in both NOESY and RFDR spectra were assigned as shown in Figure 2.

Analysis of NOE and RFDR Buildup Curves. In order to quantify dipolar couplings and obtain proton–proton distances, it is important to understand the exchange of proton magnetization via incoherent NOE cross-relaxation effect in NOESY and coherent $^1H-^1H$ dipolar cuplings recovered under MAS. In the RFDR pulse sequence, a series of rotor-synchronized 180° pulses, that is, one inversion pulse per rotor period, was used to recover the $^1H-^1H$ dipolar couplings. Since the NOE effect was not affected by the 180° pulses in the RFDR sequence, it was also observed in 2D $^1H/^1H$ RFDR spectra. Therefore, the cross peak intensities in the 2D $^1H/^1H$

dx.doi.org/10.1021/jp4034003 | J. Phys. Chem. B XXXX, XXX, XXX–XXX

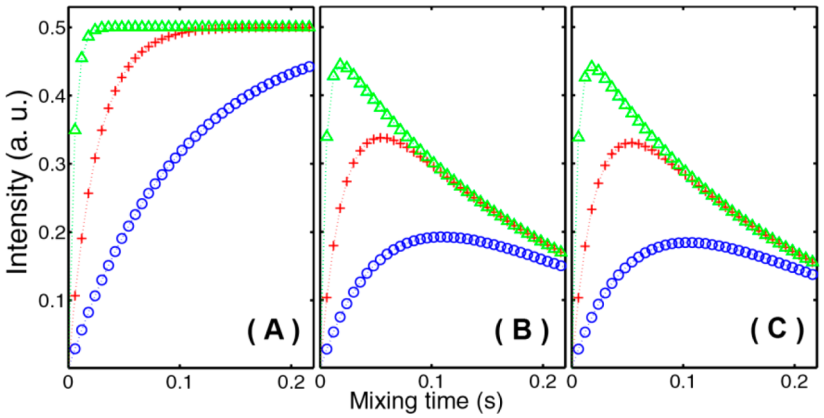

Figure 3. Simulated buildup curves of the cross peak intensities between two spins that have a cross-relaxation rate R of 5 s^{-1} (○), 20 s^{-1} (+) and 100 s^{-1} (Δ). In the simulation, the T_1 relaxation of the spins was set to 0.5 s. In panel C, the excitation efficiency of the 180° was set to 99.8% with T_1 = 0.5 s. The T_1 relaxation was set to 0.5 s in (A), while in (B) the signal attenuation by the loss of the peak intensity due to the pulse imperfection in RFDR was considered, that is, P_{180} = 99.8%. (C) The buildup curves for NOESY with T_1 = 0.1 s; other parameters are identical to that used for A.

RFDR spectra arise from two differenct interactions: NOE cross-relaxation effect and the spin diffusion via dipoalr couplings. Therefore, the time dependence of the cross peak intensity can be described by the following linear differential equation using kinetic matrices **R** and **L**[26−28]

$$\frac{d\mathbf{M}}{dt} = [\mathbf{R} + \mathbf{L}]\cdot\mathbf{M} \tag{1}$$

Within the matrix **R**, the element R_{ii} is the autorelaxation rate of spin I, while R_{ij} represents the cross-relaxation rate between spins i and j, and can be written as[3,29]

$$R_{ij} = -\left(\frac{a_H}{r_{ij}^6}\right)(6J(2\omega) - J(0)) \tag{2}$$

where $a_H = 5.6965 \times 10^{10}$ Å^6 s^{-1} is the ^{1}H−^{1}H dipolar coupling constant, r_{ij} is the distance between spins i and j, J_n is the spectral density function, and ω is the spectral frequency of the nuclei. The element $L_{ij} = D_{ij}/r_{ij}^2$ is the magnetization transfer between spins i and j, and D is the diffusion constant. The elements L_{ij} are included to account for the additional magnetization exchange process due to the dipolar couplings among nuclear spins. The diffusion constant D accounts for the averaged effect from spins located at long distances. The interactions among nearby nuclear spins are given by the term R_{ii}. The NOESY and RFDR buildup calculations were performed using a diagonalization scheme.[30] The buildup curves were calculated using a script written in Matlab and are given in Figure 3 and the values for the parameters used in the simulations are given in Table 1. The difference between the 2D NOESY and RFDR spectra gives the cross peaks that arise only from the spin diffusion due to ^{1}H−^{1}H dipolar couplings.

In the 2D ^{1}H/^{1}H RFDR spectrum, the observed cross peak intensities were also affected by the inversion efficiency of 180° pulse besides the T_1 relaxation effect, as a large number of 180° pulses were used in the mixing period of the sequence. If the inversion efficiency of the 180° pulse is 99.9%, then after a 100 ms mixing time consisting of 270 π pulses under a spinning speed of 2.7 kHz, the total signal can be estimated to be 0.999^{270} = 76% of the initial signal. The loss of the peak intensity due to the pulse imperfection can be simulated using the following equation

Table 1. The Best-Fitting Parameters for the Buildup Curves Observed from RFDR and NOESY Spectra[a]

	RFDR buildup curve			NOESY buildup curve		
residues	$1/T_1$*	R	I_0	$1/T_1$*	R	I_0
F5HAHB	3.5	22	10.5	2	5	2
A9HAHB	9	6	135	2.5	4	21
K10HAHB	3	4	9.5	2.5	4	2
F12HAHB	6	22	22	2	5	3
A15HAHB	9	6	200	2.5	4	23
F16HAHB1	8	22	26	2	5	3
V17HAHB	8	70	20	2	5	6
L20HAHB	6	70	16.5	2	5	6.5
K21HAHB1	4	24	24	1.5	4	13
L6HAHD1	3	3	31	1.5	1.5	17
V17HAHD1	7	4	105	2.5	1	63
L20HAHD	6	4	110	2.5	1	59

[a]Where T_1* is the observed relaxation time, which includes the pulse imperfection in RFDR. R is the buildup rate and I_0 is the peak intensity.

$$I = I_0(P_{180})^{t_{mix}*\omega_r} \tag{3}$$

Where P_{180} is the inversion efficiency of 180° pulses and ω_r is the spinning speed of the sample.

For a two spin-1/2 system, the simulated buildup curve for RFDR is shown in Figure 3. In this simulation, the buildup rate was set to 5, 20, and 100 s^{-1}. The T_1 relaxation was set to 0.5 s in Figure 3A, while in Figure 3B the signal attenuation by the loss of the peak intensity due to the pulse imperfection in RFDR was considered, that is, P_{180} = 99.8%. From the simulation, it can be seen that the signal attenuation due to the pulse imperfection is an exponential decay like the relaxation effect, which can be explained by using the following equation when the inversion efficiency P_{180} is close to 1

$$\begin{aligned} I &= I_0(P_{180})^{t_{mix}*R_{MAS}} \\ &\approx I_0[1 - t_{mix}*R_{MAS}(1 - P_{180})] \\ &\approx \exp I_0[-t_{mix}*R_{MAS}(1 - P_{180})] \end{aligned} \tag{4}$$

R_{MAS} is the magic angle spinning speed of the sample (in Hz). Therefore, the effect of the pulse imperfection can be included in the relaxation terms and will not be discussed separately.

dx.doi.org/10.1021/jp4034003 | J. Phys. Chem. B XXXX, XXX, XXX−XXX

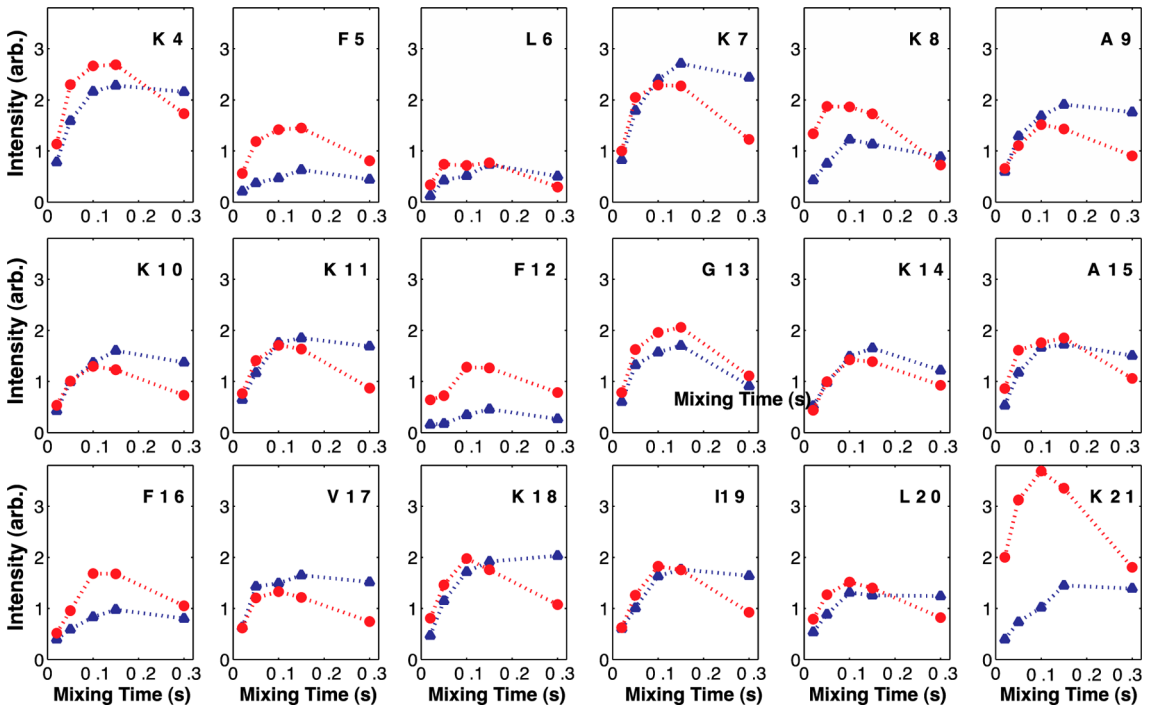

Figure 4. Experimentally measured buildup curves of the RFDR (red) and NOESY (blue) cross peaks between amide-NH and H_a nuclei for residues of MSI-78 embedded in perpetuated DPC micelles. The intensity scales were arbitrarily chosen but were set identical for all buildups to enable a direct comparison. RFDR and NOESY spectra were obtained for five different mixing times of 20, 50, 100, 150, and 300 ms.

When finite 180° pulses are applied in the RFDR pulse sequence, the restored dipolar coupling interaction will be similar to that for a static spin system. A larger duty factor, that is, the ratio between the 180° pulse width and the rotor period, can enhance the effective dipolar coupling recovered by the RFDR pulse sequence. Therefore, applying adiabatic pulses during the RFDR mixing period could improve the dipolar recoupling efficiency.[31,32] For a given limited RF power level, adiabatic pulses could provide a higher inversion efficiency for the 180° pulses during the RFDR mixing time than the standard hard 180° pulses. However, the duration of an adiabatic inversion pulse (>100 μs) is much longer than that of a hard 180° pulse (3 μs) used in this study. Therefore, the use of a long adiabatic pulse train could generate significant heating, when the RFDR mixing time is >100 ms. Therefore, in this study, we used hard 180° pulses as it enables the use of high power pulses.

Comparison of Cross Peak Intensities Observed in 2D RFDR and NOESY Spectra. 2D ^{1}H/^{1}H NOESY and RFDR spectra obtained under MAS from DPC micelles containing MSI-78 are very similar in the amide-proton region (7−9 ppm) due to the weak residual proton−proton dipolar couplings. This is evident from NOE and RFDR buildup curves shown for the amide-HN and H_α cross peaks in Figure 4. A significant difference between these two buildup curves was observed for a longer mixing time where the RFDR cross peak intensities decreased significantly due to the imperfection of 180° pulses. On the other hand, for a short mixing time (<100 ms), the RFDR and NOESY buildup curves are very similar for most of the amino acid residues (see Figure 4). This observation suggests that the residual ^{1}H−^{1}H dipolar couplings associated with the amide protons in the sample are negligible. In order to determine the crosspeaks associated with residual ^{1}H−^{1}H dipolar couplings, a difference 2D spectrum was obtained by subtracting the 2D NOESY spectrum from the 2D RFDR spectrum obtained using the same mixing time of 100 ms. Since the cross peaks in RFDR spectra arise from the combined effects of dipolar coupling and NOE, the buildup rate should be higher for RFDR spectra than that of NOESY; this should generate a larger peak intensity in 2D RFDR spectra as shown in the simulation (Figure 3) and experimental results (Figure 4). The difference between the cross peak intensities observed in RFDR and NOESY spectra reaches a maximum value at a mixing time of 100 ms as seen from the buildup curves for most residues in Figure 4. For mixing times longer than 100 ms, the peak intensity observed from RFDR was attenuated due to the imperfection of the applied 180° pulses, which reduced the observed intensity difference between RFDR and NOESY spectra. The sum and difference of RFDR and NOESY spectra obtained with a 100 ms mixing time are presented in Figure 5. To avoid any potential experimental artifacts, the 2D experiments were performed by recording the odd t1 slices as RFDR and even slices as NOESY.

Weak Dipolar Couplings Observed in the Backbone Amide-Region of MSI-78. Since the highly cationic MSI-78 peptide could weakly bind with zwitterionic DPC micelles and well exposed to the bulk water, ^{1}H−^{1}H dipolar couplings could have been significantly suppressed for most residues in the peptide.[33] As a result, only few cross peaks, such as K21H-HA and K21HA-HB, were observed in the fingerprint region of the difference 2D spectrum (Figure 5). This observation indicates that K21 has a strong electrostatic interaction with the phosphate group of the DPC headgroup in micelles, which could prevent the complete averaging of the ^{1}H−^{1}H dipolar interaction associated with this residue. Some protons from the side chains were also observed in Figure 5, such as L6H−K7ζ. Some backbone protons, such as F5 and F16, also exhibited slightly higher signal intensity in RFDR than in NOESY as seen

dx.doi.org/10.1021/jp4034003 | J. Phys. Chem. B XXXX, XXX, XXX−XXX

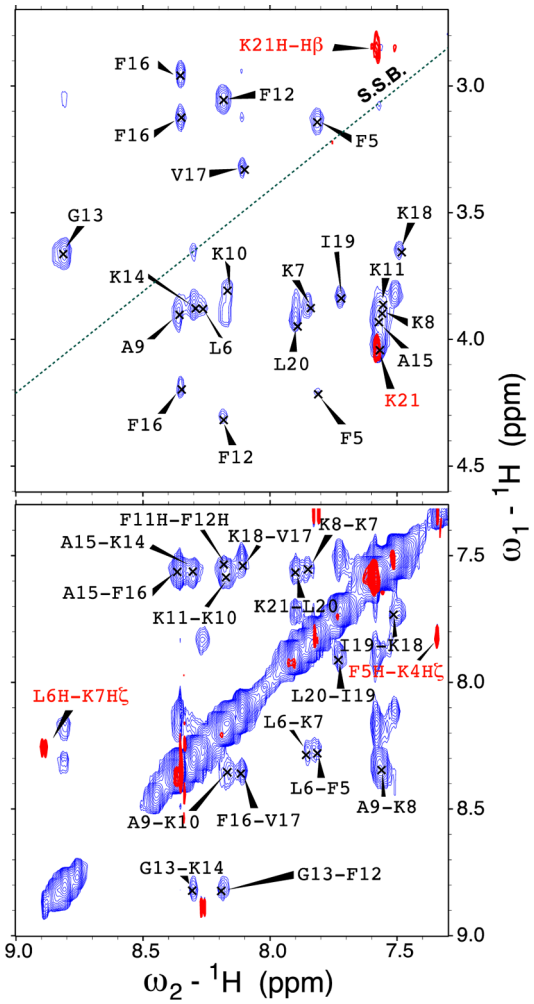

Figure 5. The sum (blue) and difference (red) 2D ^{1}H/^{1}H chemical shift correlation spectra obtained from 2D RFDR and NOESY spectra obtained using a mixing time of 100 ms. All other experimental conditions are as mentioned in the Figure 4 caption.

in Figure 4. This could be because these two residues are located in the dimeric interface of the MSI-78 peptide.[34] These results suggest that only a limited number of ^{1}H−^{1}H dipolar coupling constraints can be measured in the backbone region for a weakly membrane-bound peptide. Nevertheless, a large number of NOE constraints can be obtained from 2D RFDR spectra obtained under MAS, just like in the case of solution NMR experiments, demonstrating the feasibility of structure determination for such systems.

Strong Dipolar Couplings Observed in the Side Chain Region. The buildup rates associated with the cross peaks in the H_α and the side chain regions of 2D ^{1}H/^{1}H chemical shift correlation spectra obtained using RFDR and NOESY are shown in Figure 6. The results show that the buildup rates observed for RFDR are significantly higher than that for NOESY. The RFDR buildup rate reaches a maximum intensity within 100 ms for most residues and it is within 20 ms for some residues (for example, the cross peaks of V17HAHB and L20HAHB). The maximum intensity of the cross peaks observed in RFDR is 3−8 times stronger than that in NOESY. The buildup curves were simulated using eq 1. The simulated results are plotted in Figure 6 for a comparison, and the best-fitting parameters are given in Table 1. Three parameters were used in the simulations: relaxation time T_1*, buildup rate R, and peak intensity I_0. T_1* includes contributions from T_1 relaxation of protons and also the imperfection of 180° pulses used in RFDR. Therefore, T_1* values for RFDR are generally shorter than that for NOESY. The simulated buildup curves fit well with the experimental data. The intensities of the cross peaks observed in RFDR and NOESY spectra significantly differ between residues. However, the intensities of the peaks observed in RFDR spectra are all significantly higher than those observed in NOESY spectra. These results suggest that a large number of ^{1}H−^{1}H dipolar coupling constraints can be measured for the side chains, even for the weakly membrane-bound peptides, in addition to the NOE constraints that can be obtained from NOESY or RFDR experiments. Though micelles are used in this study, the approach demonstrated here is valid for most model membranes including bicelles,[7,35] liposomes (particularly SUVs, LUVs, and GUVs), nanodiscs,[36,37] lipid

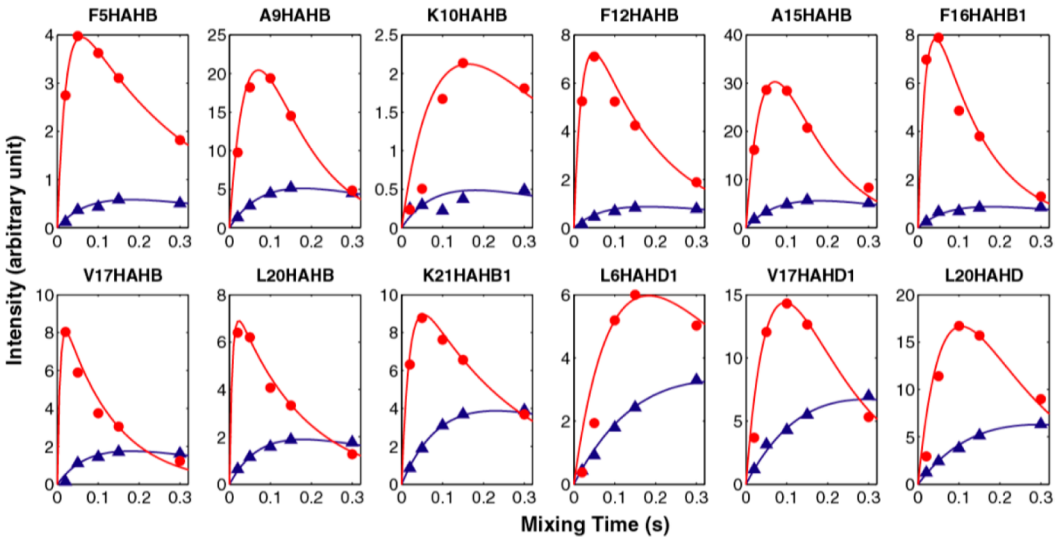

Figure 6. The buildup curves for the RFDR (red) and NOESY (blue) cross peaks between H_A and other side chain protons in the same residue are shown for each residue of MSI-78 embedded in DPC micelles. All other details are as given in the Figure 4 caption.

dx.doi.org/10.1021/jp4034003 | J. Phys. Chem. B XXXX, XXX, XXX−XXX

extracts from cells, and will also be useful for in-cell MAS and tissue metabolomics[38] studies. Therefore, 2D $^{1}H-^{1}H$ RFDR experiment can be a powerful tool to investigate a variety of biological processes including aggregation, folding, refolding, and misfolding of peptides and proteins in the membrane interface.[17,39−41]

CONCLUSION

In this study, we have demonstrated that high-resolution 2D $^{1}H/^{1}H$ chemical shift correlation spectra can be obtained using RFDR or NOESY pulse sequences under MAS for a membrane-bound antimicrobial peptide. Our simulated results are in excellent agreement with the experimentally observed buildup rates of intensities of cross peaks observed in NOESY and RFDR spectra. These results suggest that 2D $^{1}H/^{1}H$ RFDR can be used to measure residual $^{1}H-^{1}H$ dipolar couplings to determine high-resolution structure and dynamics of membrane-associated peptides without the need for the expensive isotopic labeling. The strong $^{1}H-^{1}H$ dipolar couplings observed for the side chains, even in the case of a weakly membrane-bound peptide, suggest that the 2D RFDR can be a valuable tool to monitor the membrane-interaction-induced biological properties of peptides and proteins. Multidimensional experiments can be developed using RFDR to overcome the challenges posed by large membrane proteins. In addition, the use of fast data collection approaches using paramagnetic relaxation enhancement effect[42−47] and double acquisition[48−50] would enable high-throughput solid-state NMR studies.

AUTHOR INFORMATION

Corresponding Author

*E-mail: ramamoor@umich.edu. Tel: (734)647-6572.

Notes

The authors declare no competing financial interest.

ACKNOWLEDGMENTS

This research is supported by funds from NIH (GM084018 and GM095640 to A.R.).

REFERENCES

(1) Wuthrich, K. *NMR of Proteins and Nucleic Acid*; Wiley: New York, 1986.

(2) Neuhaus, D.; Williamson, M. P. *The Nuclear Overhauser Effect in Structural and Conformational Analysis*; Wiley: New York, 2000.

(3) Cavanagh, J.; Fairbrother, W. J.; Palmer, A. G.; Rance, M.; Skleton, N. J. *Protein NMR Spectroscopy: Principles and Pratice*; Academic Press: San Diego, 2007.

(4) Prestegard, J. H.; Bougault, C. M.; Kishore, A. I. Residual dipolar couplings in structure determination of biomolecules. *Chem. Rev.* **2004**, *104*, 3519.

(5) Loquet, A.; Giller, K.; Becker, S.; Lange, A. Supramolecular Interactions Probed by 13C−13C Solid-State NMR Spectroscopy. *J. Am. Chem. Soc.* **2010**, *132*, 15164.

(6) Tjandra, N.; Bax, A. Direct measurement of distances and angles in biomolecules by NMR in a dilute liquid crystalline medium. *Science* **1997**, *278*, 1111.

(7) Dürr, U. H. N.; Gildenberg, M.; Ramamoorthy, A. The magic of bicelles lights up membrane protein structure. *Chem. Rev.* **2012**, *112*, 6054−6074.

(8) Kumar, A.; Wagner, G.; Ernst, R. R.; Wüthrich, K. Build-up Rates of the Nuclear Overhauser Effects Measured by Two-Dimensional Proton Magnetic Resonance Spectroscopy: Implications for Studies of Protein Conformation. *J. Am. Chem. Soc.* **1981**, *103*, 3654.

(9) van Buuren, B. N.; Schleucher, J.; Wittmann, V.; Griesinger, C.; Schwalbe, H.; Wijmenga, S. S. NMR spectroscopic determination of the solution structure of a branched nucleic acid from residual dipolar couplings by using isotopically labeled nucleotides. *Angew. Chem., Int. Ed.* **2004**, *43*, 187.

(10) Han, Y.; Ahn, J.; Concel, J.; Byeon, I. J.; Gronenborn, A. M.; Yang, J.; Polenova, T. Solid-State NMR Studies of HIV-1 Capsid Protein Assemblies. *J. Am. Chem. Soc.* **2010**, *132*, 1976.

(11) Rienstra, C. M.; Tucker-Kellogg, L.; Jaroniec, C. P.; Hohwy, M.; Reif, B.; McMahon, M. T.; Tidor, B.; Lozano-Perez, T.; Griffin, R. G. *de novo* determination of peptide structure with solid-state magic-angle spinning NMR spectroscopy. *Proc. Natl. Acad. Sci. U.S.A.* **2002**, *99*, 10260.

(12) Franks, W. T.; Zhou, D. H.; Wylie, B. J.; Money, B. G.; Graesser, D. T.; Frericks, H. L.; Sahota, G.; Rienstra, C. M. Magic-Angle Spinning Solid-State NMR Spectroscopy of the Beta1 Immunoglobulin Binding Domain of Protein G (GB1): ^{15}N and ^{13}C Chemical Shift Assignments and Conformational Analysis. *J. Am. Chem. Soc.* **2005**, *127*, 12291.

(13) Siemer, A. B.; Huang, K. Y.; McDermott, A. E. Protein-ice interaction of an antifreeze protein observed with solid-state NMR. *Proc. Natl. Acad. Sci. U.S.A.* **2010**, *107*, 17580.

(14) *NMR Spectroscopy of Biological Solids*; Ramamoorthy, A., Ed.; Taylor & Francis: New York, 2006.

(15) Banci, L.; Bertini, I.; Blaževitš, O.; Cantini, F.; Lelli, M.; Luchinat, C.; Mao, J.; Vieru, M. NMR Characterization of a "Fibril-Ready" State of Demetalated Wild-Type Superoxide Dismutase. *J. Am. Chem. Soc.* **2011**, *133*, 345−9.

(16) Ramamoorthy, A. Beyond NMR spectra of antimicrobial peptides: Dynamical images at atomic resolution and functional insights. *Solid State Nucl. Magn. Reson.* **2009**, *35*, 201−207.

(17) Brender, J.; Salamekh, S.; Ramamoorthy, A. Membrane-Disruption and Early Events in the Aggregation of the Diabetes Related Peptide IAPP from a Molecular Perspective. *Acc. Chem. Res.* **2012**, *116*, 3650−3658.

(18) Braunschweiler, L.; Ernst, R. R. Coherence transfer by isotropic mixing: application to proton correlation spectroscopy. *J. Magn. Reson.* **1983**, *53*, 521.

(19) Lipsky, B. A.; Holroyd, K. J.; Zasloff, M. opical versus systemic antimicrobial therapy for treating mildly infected diabetic foot ulcers: arandomized, controlled, double-blinded, multicenter trial of pexiganan cream. *Clin. Infect. Dis.* **2008**, *47*, 1537−45.

(20) Maloy, W. L.; Kari, U. P. Structure-activity studies on magainins and other host defense peptides. *Biopolymers* **1995**, *37*, 105−22.

(21) Gottler, L. M.; Ramamoorthy, A. Membrane Orientation, Mechanism, and Function of Pexiganan - A Highly Potent Antimicrobial Peptide Designed From Magainin. *Biochim. Biophys. Acta, Biomembr.* **2009**, *1788*, 1680−6.

(22) Bennett, A. E.; Griffin, R. G.; Ok, J. H.; Vega, S. Chemical shift correlation spectroscopy in rotating solids: Radio frequency-driven dipolar recoupling and longitudinal exchange. *J. Chem. Phys.* **1992**, *96*, 8624.

(23) Aucoin, D.; Camenares, D.; Zhao, X.; Jung, J.; Sato, T.; Smith, S. O. High-resolution 1H MAS RFDR NMR of biological membranes. *J. Magn. Reson.* **2009**, *197*, 77.

(24) Delaglio, F.; Grzesiek, S.; Vuister, G. W.; Zhu, G.; Pfeifer, J.; Bax, A. NMRPipe: a multidimensional spectral processing system based on UNIX pipes. *J. Biomol. NMR* **1995**, *6*, 277.

(25) Goddard, T. D.; Kneller, D. G. *SPARKY 3*; University of California: San Francisco.

(26) Abragam, A. *Principles of Nuclear Magnetism*; Oxford University Press: Oxford, 1986.

(27) Bloom, M.; Reeves, L. W.; Wells, E. J. Spin Echoes and Chemical Exchange. *J. Chem. Phys.* **1965**, *42*, 1615.

(28) McConnell, H. M. Reaction Rates by Nuclear Magnetic Resonance. *J. Chem. Phys.* **1965**, *28*, 430.

(29) Vogeli, B.; Segawa, T. F.; Leitz, D.; Sobol, A.; Choutko, A.; Trzesniak, D.; van Gunsteren, W.; Riek, R. Exact Distances and

Internal Dynamics of Perdeuterated Ubiquitin from NOE Buildups. *J. Am. Chem. Soc.* **2009**, *131*, 17215.
(30) Schmidt-Rohr, K.; Spiess, H. W. *Multidimensional Solid-State NMR and Polymers*; Academic Press: New York, 1994.
(31) Heise, B.; Leppert, J.; Ohlenschager, O.; Gorlach, M.; Ramachandran, R. Chemical shift correlation via RFDR: elimination of resonance offset effects. *J. Biomol. NMR* **2002**, *24*, 237.
(32) Leppert, J.; Heise, B.; Ohlenschlager, O.; Gorlach, M.; Ramachandran, R. Broadband RFDR with adiabatic inversion pulses. *J. Biomol. NMR* **2003**, *26*, 13.
(33) Hallock, K. J.; Lee, D. K.; Ramamoorthy, A. MSI-78, an analogue of the magainin antimicrobial peptides, disrupts lipid bilayer structure via positive curvature strain. *Biophys. J.* **2003**, *84*, 3052.
(34) Porcelli, F.; Buck-Koehntop, B. A.; Thennarasu, S.; Ramamoorthy, A.; Veglia, G. Structures of the Dimeric and Monomeric Variants of Magainin Antimicrobial Peptides (MSI-78 and MSI-594) in Micelles and Bilayers by NMR Spectroscopy. *Biochemistry* **2006**, *45*, 5793.
(35) Dürr, U. H. N.; Soong, R.; Ramamoorthy, A. When the detergent meets bilayer: Birth and coming of age of lipid bicelles. *Prog. NMR Spectrosc.* **2013**, *69*, 1−22.
(36) Kijac, A.; Shih, A. Y.; Nieuwkoop, A. J.; Schulten, K.; Sligar, S. G.; Rienstra, C. M. Lipid-Protein Correlations in Nanoscale Phospholipid Bilayers Determined by Solid-State Nuclear Magnetic Resonance. *Biochemistry* **2010**, *49*, 9190−8.
(37) Hyberts, S. G.; Etzkorn, M.; Raschle, T.; Wagner, G. Optimized Phospholipid Bilayer Nanodiscs Facilitate High-Resolution Structure Determination of Membrane Proteins. *J. Am. Chem. Soc.* **2013**, *135*, 1919−25.
(38) Somashekar, B.; Kamarajan, P.; Danciu, T.; Kapila, Y.; Chinnaiyan, A.; Rajendiran, T.; Ramamoorthy, A. Magic Angle Spinning NMR Based Metabolic Profiling of Head and Neck Squamous Cell Carcinoma Tissues. *J. Prot. Res.* **2011**, *10*, 5232−5241.
(39) Dürr, U. H. N.; Waskell, L.; Ramamoorthy, A. The cytochromes P450 and b5 and their reductases—Promising targets for structural studies by advanced solid-state NMR spectroscopy. *Biochim. Biophys. Acta, Biomembr.* **2007**, 3235−3259.
(40) Ramamoorthy, A. Beyond NMR spectra of antimicrobial peptides: Dynamical images at atomic resolution and functional insights. *Solid State Nucl. Magn. Reson.* **2009**, *35*, 201−207.
(41) Barrett, P. J.; Chen, J.; Cho, M. K.; Kim, J. H.; Lu, Z.; Mathew, S.; Peng, D.; Song, Y.; Van Horn, W. D.; Zhuang, T.; Sönnichsen, F. D.; Sanders, C. R. The Quiet Renaissance of Protein Nuclear Magnetic Resonance. *Biochemistry* **2013**, *52*, 1303−20.
(42) Ganapathy, S.; Naito, A.; McDowell, C. A. Paramagnetic Doping As an Aid in Obtaining High-Resolution Carbon-13 NMR Spectra of Biomolecules in the Solid State. *J. Am. Chem. Soc.* **1981**, *103*, 6011−6015.
(43) Wickramasinghe, N. P.; Kotecha, M.; Samoson, A.; Past, J.; Ishii, Y. Sensitivity enhancement in 13C solid-state NMR of protein microcrystals by use of paramagnetic metal ions for optimizing 1H T1 relaxation. *J. Magn. Reson.* **2007**, *184*, 350−356.
(44) Yamamoto, K.; Xu, J.; Kawulka, K. E.; Vederas, J. C.; Ramamoorthy, A. Use of a Copper-Chelated-Lipid Speeds Up NMR Measurements From Membrane Proteins, A. *J. Am. Chem. Soc.* **2010**, *132*, 6929−31.
(45) Yamamoto, K.; Vivekanandan, S.; Ramamoorthy, A. Fast NMR Data Acquisition from Bicelles Containing a Membrane-Associated Peptide at Natural-Abundance. *J. Phys. Chem. B* **2011**, *115*, 12448−55.
(46) Nadaud, P. S.; Helmus, J. J.; Sengupta, I.; Jaroniec, C. P. Rapid Acquisition of Multidimensional Solid-State NMR Spectra of Proteins Facilitated by Covalently Bound Paramagnetic Tags. *J. Am. Chem. Soc.* **2010**, *132*, 9561−9563.
(47) Tang, M.; Berthold, D. A.; Rienstra, C. M. Solid-State NMR of a Large Membrane Protein by Paramagnetic Relaxation Enhancement. *J. Phys. Chem. Lett.* **2011**, *2*, 1836−1841.
(48) Gopinath, T.; Veglia, G. Orphan spin operators enable the acquisition of multiple 2D and 3D magic angle spinning solid-state NMR spectra. *J. Chem. Phys.* **2013**, *138*, 184201.
(49) Gopinath, T.; Veglia, G. 3D DUMAS: Simultaneous Acquisition of Three Dimensional Magic Angle Spinning Solid State NMR Experiments of Proteins. *J. Magn. Reson.* **2012**, *220*, 79−84.
(50) Gopinath, T.; Veglia, G. Dual Acquistion Magic-Angle Spinning Solid State NMR-Spectroscopy: Simultaneous Acquisition of Multidimensional Spectra of Biomolecules. *Angew. Chem., Int. Ed.* **2012**, *51*, 2731−2735.